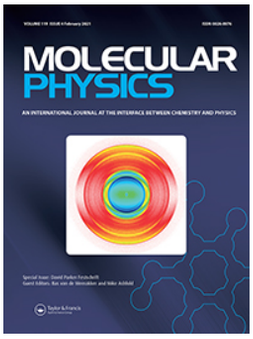

Taylor & Francis
Taylor & Francis Group

Molecular Physics

An International Journal at the Interface Between Chemistry and Physics

ISSN: (Print) (Online) Journal homepage: https://www.tandfonline.com/loi/tmph20

Non-adiabatic coupling as a frictional force in (He, H, H)$^+$ dynamics and the formation of HeH_2^+

Satyam Ravi, Soumya Mukherjee, Bijit Mukherjee, Satrajit Adhikari, Narayanasami Sathyamurthy & Michael Baer

To cite this article: Satyam Ravi, Soumya Mukherjee, Bijit Mukherjee, Satrajit Adhikari, Narayanasami Sathyamurthy & Michael Baer (2021) Non-adiabatic coupling as a frictional force in (He, H, H)$^+$ dynamics and the formation of HeH_2^+, Molecular Physics, 119:4, e1811907, DOI: 10.1080/00268976.2020.1811907

To link to this article: https://doi.org/10.1080/00268976.2020.1811907

View supplementary material

Published online: 01 Sep 2020.

Submit your article to this journal

Article views: 121

View related articles

View Crossmark data

Citing articles: 2 View citing articles

Full Terms & Conditions of access and use can be found at
https://www.tandfonline.com/action/journalInformation?journalCode=tmph20

MOLECULAR PHYSICS
2021, VOL. 119, NO. 4, e1811907 (18 pages)
https://doi.org/10.1080/00268976.2020.1811907

Taylor & Francis
Taylor & Francis Group

RESEARCH ARTICLE

Check for updates

Non-adiabatic coupling as a frictional force in (He, H, H)$^+$ dynamics and the formation of HeH_2^+

Satyam Ravi[a], Soumya Mukherjee[a], Bijit Mukherjee[a], Satrajit Adhikari[a], Narayanasami Sathyamurthy[b] and Michael Baer[c]

[a]School of Chemical Sciences, Indian Association for the Cultivation of Science, Kolkata, India; [b]Department of Chemistry, Indian Institute of Technology Kanpur, Kanpur, India; [c]The Fritz Haber Center for Molecular Dynamics, The Hebrew University of Jerusalem, Jerusalem, Israel

ABSTRACT

It is shown that the Born–Oppenheimer–Huang non-adiabatic coupling terms (NACTs) in a molecular Hamiltonian can be considered as equivalent to a friction force in classical mechanics and consequently responsible for the formation of triatomic species like HeH_2^+. The classical equation of motion is solved accordingly for a test case of a helium atom approaching an H_2^+ molecule at its potential minimum along the collinear axis and lines parallel to it and also for the C_{2v} geometry. It is shown that the singular NACTs between the first two excited states slow down the motion of the three quasi-ions (He, H, H)$^+$ while approaching each other and result in substantial loss of kinetic energy in the collision process. These results have profound implications for the formation of di- and triatomic species in the early universe, during the chemical synthesis epoch following the nucleosynthesis that followed the Big Bang.

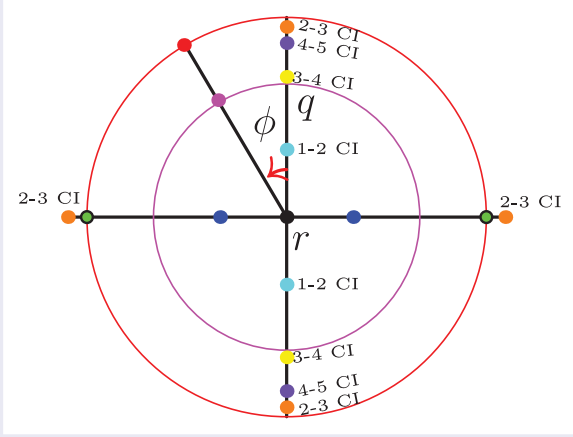

ARTICLE HISTORY
Received 29 June 2020
Accepted 10 August 2020

KEYWORDS
Non-adiabatic coupling; astrochemistry; molecular processes; ISM molecules

1. Introduction

The current understanding of the early universe [1–3] is that chemical synthesis followed nucleosynthesis after the Big Bang, with the formation of neutral H, He and Li atoms. The first diatomic species formed was perhaps HeH^+ through radiative association:

$$He + H^+ \rightarrow HeH^+ + h\nu. \quad \text{(R1)}$$

The rate of forming HeH^+ through an alternative channel

$$He^+ + H \rightarrow HeH^+ + h\nu. \quad \text{(R2)}$$

seems to be several orders of magnitude less for red shift $z > 1000$.

The rate of the reaction

$$He + H_2^+ \rightarrow HeH^+ + H \quad \text{(R3)}$$

CONTACT Narayanasami Sathyamurthy nsath@iitk.ac.in

Supplemental data for this article can be accessed here. https://doi.org/10.1080/00268976.2020.1811907

© 2020 Informa UK Limited, trading as Taylor & Francis Group

seems to be even less for $2000 < z < 200$. The reverse of reaction (R2)

$$\mathrm{HeH^+} + h\nu \rightarrow \mathrm{He^+} + \mathrm{H} \tag{R4}$$

seems to have depleted $\mathrm{HeH^+}$ for $z > 200$. In other words, reaction (R2) was a reversible process for $z > 200$.

The chemical reaction

$$\mathrm{HeH^+} + \mathrm{H} \rightarrow \mathrm{He} + \mathrm{H_2^+} \tag{R5}$$

seems to have played an important role in depleting $\mathrm{HeH^+}$ for $200 < z < 10$. The dissociative recombination (DR)

$$\mathrm{HeH^+} + e \rightarrow \mathrm{He} + \mathrm{H} \tag{R6}$$

is believed to be a competing channel for reducing the population of $\mathrm{HeH^+}$ in recent times ($10 < z < 1$). A quantitative comparison of the production and destruction rates of $\mathrm{HeH^+}$ through different channels is given in Figure 2 of Ref. [4]. Interestingly, the first observation [5] of $\mathrm{HeH^+}$ and $\mathrm{HeH_2^+}$ in the laboratory was using mass spectrometry, as early as 1925. But, only recently, Güsten *et al.* [6] reported detection of $\mathrm{HeH^+}$ in the planetary nebula NGC 7027 through the recording of the spectrum of the $j = 1 \rightarrow 0$ ground state rotational transition providing the *long awaited confirmation* of the formation of $\mathrm{HeH^+}$ in the early universe. Güsten *et al.* [6] point out that the rate of radiative association in case of (R2) is $\sim (1.4 - 6) \times 10^{-16}\ \mathrm{cm^3\ s^{-1}}$ in the temperature range 5000–20,000 K and the rate of dissociative recombination in case of (R6) is $\sim 3.0 \times 10^{-10}\ \mathrm{cm^3\ s^{-1}}$ at 10,000 K indicating that $\mathrm{HeH^+}$, formed by the reaction (R2) would be depleted by the reaction (R6). This implies that the observed signal for $\mathrm{HeH^+}$ is much more than what is predicted by the reactions (R2)–(R6).

Novotny *et al.* [7] conclude from experiments using cryogenic ion storage ring and merged electron beam that the DR rate used by Güsten *et al.* is consistent with their observation. Therefore, there is a need to identify additional channels of $\mathrm{HeH^+}$ formation.

Although 3-body collisions are generally less frequent than 2-body collisions, Palla *et al.* [8] pointed out that under collapsing hydrogen cloud conditions in which the particle density was greater than $10^8/\mathrm{cm^3}$, three body collisions could be considered. Even though they did not consider helium in their study, 'since it is chemically inert', the possibility of helium combining with H and $\mathrm{H^+}$ to form $\mathrm{HeH_2^+}$ was very much there. Particularly since the abundance of hydrogen and helium under those conditions [9] was in the ratio 10:1, it is proposed in this paper that helium and hydrogen nuclei under the influence of electronic clouds could have formed $[\mathrm{HeH_2^+}]^*$ in its multiple electronic states stabilised by non-adiabatic coupling terms (NACTs) acting as some kind of a frictional force. They, in turn, could emit photons and come to lower energy states and also dissociate to form $\mathrm{HeH^+} + \mathrm{H}$ as well as $\mathrm{He} + \mathrm{H_2^+}$ [10–12].

Interestingly, the formation of $\mathrm{H_3^+}$ in the early universe seems to have been accounted for [1–3] and we have proposed [13–15] that its stability arises from the NACTs. Zicler *et al.* [16] had proposed the formation of $\mathrm{HeH_3^+}$ through the reaction:

$$\mathrm{He} + \mathrm{H_3^+} \rightarrow \mathrm{HeH_3^+}. \tag{R7}$$

The authors discounted the formation $\mathrm{HeH_2^+} + \mathrm{H}$ because the channel is a few eV higher in energy.

In this publication we consider for the first time the possibility that $\mathrm{HeH_2^+}$ was created in the early universe. There is no report of the detection of $\mathrm{HeH_2^+}$ in the interstellar media so far in the literature. But, that does not mean that it could not be formed for a short time and then dissociate via one, or more, of the four possible given processes:

$$\mathrm{HeH_2^+} \rightarrow \begin{cases} \mathrm{He^+} + \mathrm{H_2} & \text{(A1)} \\ \mathrm{He} + \mathrm{H_2^+} & \text{(A2)} \\ \mathrm{HeH^+} + \mathrm{H} & \text{(A3)} \\ \mathrm{He} + (\mathrm{H} + \mathrm{H})^+ & \text{(A4)} \end{cases}$$

According to this scheme we encounter creations of, eventually, three different diatomic molecules. However, reaction (A1) is not likely to happen because of its exceptionally high endothermicity and out of the two other reactions the reaction (A2) seems more promising because of its larger exothermicity and the reaction (A3) is slowed down due to the barrier formed by the endothermicity.

The first (microwave) spectral evidence for $\mathrm{HeH_2^+}$ under laboratory conditions came from ion beam experiments in which mass selected ions were subjected to microwave radiation, in the presence of electric and magnetic fields [17].

While a doublet was recorded around 21.8 GHz, with a spacing of 44.1 MHz, a sextet was recorded around 15.2 GHz with a total spread of 13.2 MHz at low power and a second sextet with a spread of 16.8 MHz at a higher power. There were noticeable differences between o-$\mathrm{H_2}$ and p-$\mathrm{H_2}$ in the spectrum of the $\mathrm{He} \cdots \mathrm{H_2^+}$ complex. There was a third resonance observed at 22.5 GHz and there were additional resonances observed in the range 123–168 GHz. Quantum chemistry studies indicate that these three quasi-ions (A4) can form a potential well as deep as -0.37 eV in the ground electronic state, relative to well separated He and $\mathrm{H_2^+}$. The well can support many bound states, with the lowest corresponding to

$D_0 = 2481\,\mathrm{cm}^{-1}$ for zero angular momentum [18–27]. Time-dependent quantum mechanical wave packet studies have shown that there are several quasi-bound states as well [28].

Recently, we started to study, topologically, molecular systems created in the early universe [13–15]. For this purpose, we considered three molecular systems, namely, H_3^{++}, H_3^{+} and H_3, and argued how H_3^{+} could be formed but not H_3 and H_3^{++}.

This study was done by considering a plane defined by the positions in the configuration space (CS) of the three quasi-ions [29] that build-up the molecular system and calculating the required Born–Oppenheimer–Huang (BOH) [30–37] non-adiabatic coupling terms (NACTs) designated as $\boldsymbol{\tau}_{\phi \mathrm{jj}+1}(\phi|q,\ \mathbf{s})$). Here, $\mathbf{s}$ stands for the spatial coordinates of the three quasi-ions (see Figure 1) and (ϕ, q) are polar coordinates to describe the distribution of the NACTs for a given situation in that plane. The tri-atomic NACTs are known to become singular at certain points known as Conical Intersections (*ci*s) [33]. The number of *ci*s is determined by various parameters that define the system, among them, the number of electronic states included in the study. Usually any two consecutive adiabatic states have at least one (common) singular point. The present study considers NACTs associated with three or more lowest electronic states to achieve better converged results. In most cases, the *ci*s are located at the *equilateral* positions of the (tri-atomic) system and occasionally at the *isosceles* positions.

As it was mentioned earlier, we are interested in the way molecules could have been formed in the early universe by free quasi-atoms wrapped by an electronic cloud.

In previous articles [13–15], it was suggested that NACTs were associated with features that enabled the creation of molecules directly from the free quasi-atoms in extreme *unfriendly* conditions, namely to form molecules from particles moving with enormously large velocities. This possibility was examined in detail with respect to the formation of H_3^{+}.

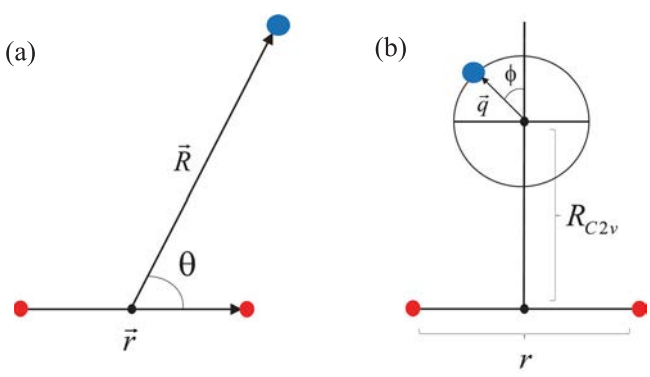

Figure 1. Schematic picture of the system of coordinates and various points of location: (a) The Jacobi system of coordinates, namely, r, R and θ; (b) The point of (1,2) or (2,3) *ci* is at $R = R_{C2v}$ and $\theta = \pi/2$, which is the centre of the circle with the radius q.

We pointed out the possibility that the NACTs were blessed with features of the kind Gell-Mann [38] and Zweig [39] attributed to their nuclear gluons. If that is the case, we could justify, at least heuristically the creation of tri-atomic molecules within the unfriendly atmosphere in the early universe.

In this paper, we present a different approach attributing dissipative features akin to that of friction to the NACTs, which could be traced to the treatment of the BOH formalism in a time-dependent framework [40] and in the semi-classical treatment of geometric phases [41].

Friction, in contrast to the conservative forces that arise from the PESs, acts directly on the velocity of the moving body to slow it down. Friction forces are discussed in various text books on Classical Mechanics [42, 43] and a typical case is a Hamiltonian of free mode vibrations affected by frictions proportional to the velocities. Consequently, in Appendix I is *derived* a classical Hamiltonian for a particle of mass m moving in a single-linear-coordinate-system $x = (-\infty, \infty)$ affected by a force derived from a potential $V(x)$ and a friction force of the kind $\beta\dot{x}$, where $\dot{x}$ is the velocity:

$$\frac{\mathrm{d}}{\mathrm{d}t}\left[\frac{m}{2}\left(\dot{x} + \frac{1}{m}\beta(x - x_0)\right)^2 + V(x)\right] = F(x, \dot{x}). \quad (1)$$

Here $F(x, \dot{x})$ is given in the form

$$F(x,\dot{x}) = (x - x_0)\left[-\frac{1}{m}\beta\frac{\mathrm{d}V}{\mathrm{d}x} + \frac{\mathrm{d}\beta}{\mathrm{d}t}\left(\frac{1}{m}\beta\,(x - x_0) + \dot{x}\right)\right] \quad (2)$$

As it may be noticed, F is actually the power reflecting the effect of the friction term in disturbing the conservation of energy of the free Hamiltonian.

Recalling the BOH equation [15,33] for a particle of mass m moving on a potential energy curve (surface) u with a total energy E and non-adiabatic coupling matrix $\boldsymbol{\tau}$,

$$-\frac{\hbar^2}{2m}\left(\nabla + \boldsymbol{\tau}\right)^2 \boldsymbol{\Psi} + (\boldsymbol{u} - E)\,\boldsymbol{\Psi} = \mathbf{0}, \quad (3)$$

where $\boldsymbol{\nabla}$ is the first order spatial derivative and $\boldsymbol{\Psi}$ is the wave function, and comparing its structure with that of Equation (1), it can be inferred that the $\boldsymbol{\tau}$ - matrix serves as a dissipative force (or a friction force). Although Equation (3) does *not seem* to include an explicit *source term* to avoid the energy loss due to friction, the conservation of energy is maintained because of the constant supply of energy by the singularity at the *ci* (it is well

known that the NACTs in Equation (3) are formed by singularities. For details, see Ref. [33]). An important feature of friction is that during the slowing down process it produces energy as heat or light - in the present case energy would be released as photons, for instance during the production of $HeH^+ + H$ and $He + H_2^+$ (as will be discussed later).

In other words, the BOH approach yields two kinds of forces, which may affect the motion of the quasi-ions: (i) One due to the PES, which has its origin in the electrostatic interaction and therefore is a relatively weak force affecting the motion of these particles within a few-eV range. (ii) The NACTs, which could be identified as (astronomical) friction that affects straightforwardly the motion of the quasi-ions while moving with high velocities.

The effect of such a friction is valid for any number of interacting quasi-ions. However it would be *inefficient* in case of two quasi-ions (because of the lack of a *ci* in such a case) but likely to be efficient in case of three or more interacting species. The reason is that the interacting quasi-ions form *ci*s at certain regions - points - in CS, which yield a distribution of highly intense NACTs, which in turn become highly intense frictions. As a result, the fast moving quasi-ions are slowed down and are forced to lose their excessive energy at a high rate and the electrostatic forces take over.

The detection of traces of HeH^+ in the Nebula NGC 7027 [6] made us to extend our studies to consider the possibility of formation of tri-atomic species like HeH_2^+, which could have served as a precursor for HeH^+ in the early universe.

The computed NACTs for H_3^+ were used to identify the equivalent friction force and the resulting classical equation of motion (Equation (1)) was solved for the centre-of-mass motion of a proton (H^+) approaching H_2 (at a fixed distance) in C_{2v} geometry for a wide range of translational energies (1–500 eV). As expected, the frictional force (arising from the NACTs) slows down the relative motion near the singularities and the possibility of trapping H_3^+ and eventual separation of H^+ and H_2 is demonstrated [44]. In the present work, we have performed classical dynamics on HeH_2^+ system in the presence of frictional forces arising from the NACTs to explore the trapping of the quasi-ions with very high kinetic energy of the incoming quasi-ion to collide with the diatom.

Thus, as was done earlier for H_3^+, we produce *circular* contours with their centres located at points along the equilateral line perpendicular to the axis formed by the two (hydrogenic) quasi-ions (see Figure 1). Along these contours are calculated the angular components of corresponding NACTs [33, Sect. 3.2.2] as a function of the angle ϕ for a given contour (namely its radius and centre). As before all these steps are undertaken with the aim of examining the possibility that the three *free* BOH quasi-ions, (He, H, H^+) can form the HeH_2^+ molecular ion.

As was mentioned earlier, the key factors to be studied in this article are the NACTs. It is well known that deriving accurate and meaningful NACTs is a long and tedious task, which requires repeated assessments and tests. One of the more crucial tests for their relevance is the fulfilment of the molecular *quantisation*, a feature frequently mentioned in our publications [13–15,33]. In general we distinguish between two-state, and multi-state results. In the present study we had to include up to four electronic states to achieve the required quantisation (see also Ref. [27]).

2. Ab initio calculations

All ab initio calculations were performed using the MOLPRO quantum chemistry package [45], where state-averaged complete active space self-consistent field (SA-CASSCF) and multi-reference configuration interaction with singles and doubles (MR-CISD) methods were employed using the aug-cc-pVTZ (AVTZ) basis set including *s*, *p*, *d* functions of H and He. Calculations of PES were carried out by MR-CISD approach, whereas the NACTs have been computed by SA-CASSCF method. We have chosen complete active space (CAS) as (4*o*, 3*e*) i.e. three electrons distributed among four active orbitals. The lowest four doublet electronic states, namely, 1^2A_1, 2^2A_1, 3^2A_1 and 4^2A_1, and the NACTs between them are calculated using MR-CISD and CASSCF methodology, respectively.

2.1. Quantisation as a probe of the relevance of the NACTs

Our ab initio calculations yield results in conformity with what have been reported earlier [18–26]. That is, HeH_2^+ in its ground electronic state is most stable in its collinear geometry $[He\text{-}H\text{-}H]^+$ with $r_{He-H} = 1.026$ Å and $r_{H-H} = 1.097$ Å and a well depth of -0.34 eV, relative to the asymptotically separated He and H_2^+ (at its potential minimum with $r_{min} = 1.054$Å). Because of the symmetry of the system, there are two potential minima (on both sides of $[H\text{-}H]^+$) as illustrated in Figure 2 for $r = 1.0$ Å.

The adiabatic potential energy values as a function of the centre-of-mass separation (R) between He and H_2^+ for the C_{2v} geometry for the ground (1) and the first two excited electronic states (2, 3) are plotted in Figure 3, along with the NACTs between

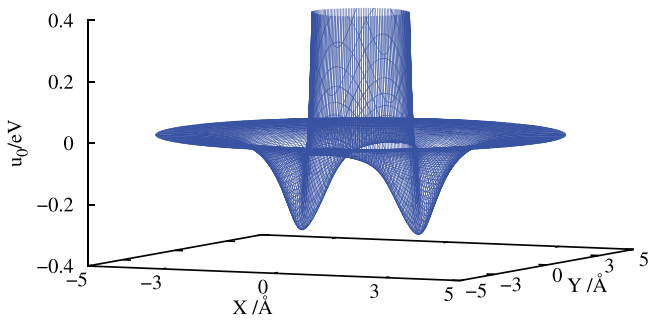

Figure 2. The adiabatic potential energy surface for the ground electronic state of the HeH_2^+ system over $X-Y$ plane, where $X = R\cos\theta$ and $Y = R\sin\theta$ for $r = 1.0$ Å. The positions of the minima for the formation of HeH_2^+ are $X = 1.5$ Å, $Y = 0$ Å and $X = -1.5$ Å, $Y = 0$ Å with well depth -0.34 eV, where the energy is scaled with respect to the asymptote of well separated He and H_2^+.

the states and the adiabatic-to-diabatic transformation (ADT) angles (see below) in a set of panels. Similar results were published for the collinear geometry in an earlier paper [27].

Each set of three panels arranged in a row relates to a given situation characterised by the geometry of the three particles: the two hydrogen nuclei are kept fixed with an internuclear distance $r = 1.0$ Å (close to their potential minimum). The helium atom is applied as a test particle so that both the adiabatic potential energy curves – APECs – (calculated as a function of R, but for a fixed angle $\theta = \pi/2$ - see Figure 1(a)) and the NACTs (calculated along circular contours defined in terms of a given radius q and given centres in CS (see Figure 1(b)) are expressed by varying its position. Thus a situation is expressed in terms of (r, θ, q) and the centre of the circle.

Following is a discussion on panels of three types: A, B, C in Figure 3: In each A-panel are given the APECs (all are identical) and the circular contours along which are calculated the NACTs. Thus, in the A-panel, the first row presents such a contour with a radius $q = 0.3$ Å and its centre at the (1,2) *ci*-point (thus, at $R = 0.54$ Å); the 2nd row displays the contour with the same centre but for a radius $q = 0.5$ Å; the 3rd row depicts the contour with the centre at $R = 1.0$ Å (thus a point in-between the (1,2) *ci*-point and the (2,3) *ci*-points) for the (same) radius ($q = 0.5$ Å) and the 4th row presents a contour with the same centre but for a radius $q = 0.7$ Å. In the B-panel, of each row are displayed the relevant NACTs, namely, $\boldsymbol{\tau}_{12}(\phi|q, \mathbf{s})$ and $\boldsymbol{\tau}_{23}(\phi|q, \mathbf{s})$ and in each C-panel the relevant ADT angles, $\boldsymbol{\gamma}_{12}(\phi|q, \mathbf{s})$ and $\boldsymbol{\gamma}_{23}(\phi|q, \mathbf{s})$, are depicted, which are expected to be quantised. In the first two C-panels, the contours surround only one *ci*, namely (1,2) *ci* but in the two lower panels, contours surround the two relevant *ci*s, namely (1,2) *ci* and (2,3) *ci*. In addition, in each of the C-panels, the value of the corresponding topological phases $\boldsymbol{\alpha}_{12}(q, \mathbf{s})$ and, $\boldsymbol{\alpha}_{23}(q, \mathbf{s})$ are given to emphasise, numerically, the extent to which these angles are quantised (the topological phases are sometimes identified with the Berry Phase) [46–55].

It is important to point out that in all four cases presented here, quantisation was achieved - sometimes with three states and sometimes with four states.

It is worth reiterating that the (angular) NACTs play the role of the astrophysical friction forces. Therefore, the NACTs should be intense enough to guarantee the frictional force to become effective in the *regions of the potential wells* to form the tri-atomic molecule. The adiabatic potential energy surface for the ground electronic state of collinear HeH_2^+ plotted in Figure 2 illustrates the relevant potential wells for $r = 1.0$ Å. Each of the two (symmetric) wells is located along the collinear axis, ~ 1 Å away from the corresponding hydrogen (see Figure 2).

In Figure 4(a), we present the planar CS, the system of coordinates, the two fixed hydrogen atoms, the helium atom rotating along two closed contours (with their centre at the origin of the system of coordinates), the position of ten *ci*s (five on each side of the collinear axis) and the position of the two potential wells.

In Figure 4(b), we display two rows of panels. In each A-panel, a circular contour is shown (one with radius $q = 1.0$ Å and the other with radius $q = 1.5$ Å) surrounding the corresponding 4 *ci*s: (1,2) *ci*, (2,3) *ci*, (3,4) *ci* and (4,5) *ci* as well as the five APECs. The two B-panels contain the NACTs $\boldsymbol{\tau}_{12}(\phi|q)$ and $\boldsymbol{\tau}_{23}(\phi|q)$and the two black$C$-panels contain the NACTs $\boldsymbol{\tau}_{34}(\phi|q)$ and $\boldsymbol{\tau}_{45}(\phi|q)$ as a function of ϕ.

It is clear from our reported results that the NACTs are distributed uniformly throughout the (planar) CS and therefore are expected to be relevant in keeping the three quasi-ions in close proximity to each other and support the potential well in building-up the HeH_2^+ molecule.

It is important to mention that the singular behaviour of the NACTs can be eliminated by adopting what is known as diabatic representation. This is accomplished by applying a unitary transformation of adiabatic electronic eigenfunction, known as the adiabatic-to-diabatic transformation (ADT) [33,36,37]. In the past few decades, numerous studies have been dedicated to understand such a transformation and apply it to construct diabatic PESs for various molecular systems. In the reference section, we have listed a series of publications which to some extent enable the reader to get acquainted with the literature of NACTs and ADT [40,56–113].

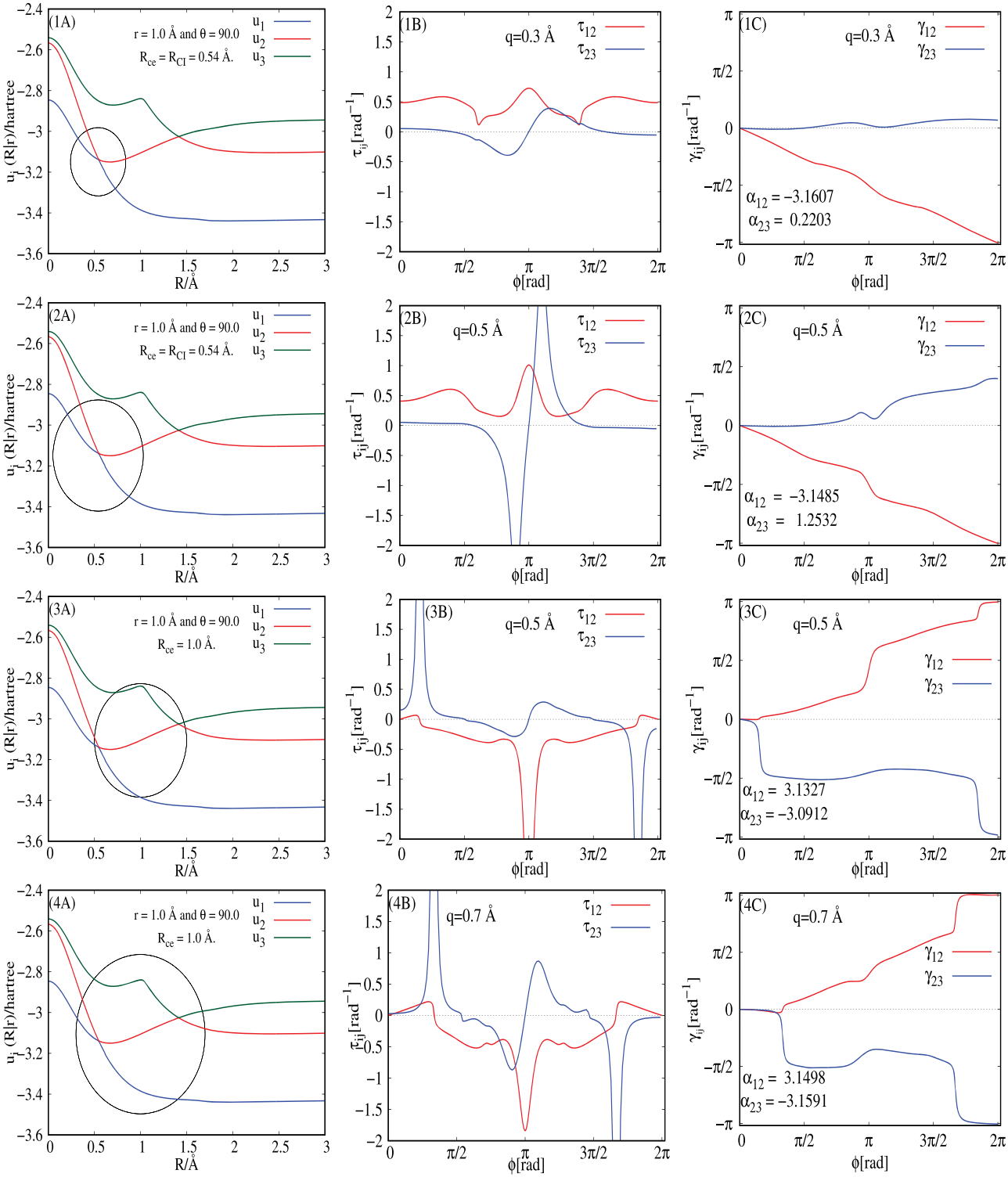

Figure 3. Results shown along contours with different centres (R_{ce}) and radii (q). Row 1: Panels (A-C) show results for HeH_2^+ calculated at $r = 1.0$ Å, $R = 0.54$ Å for radius $q = 0.3$ Å; Row 2: Panels(A–C) show results for HeH_2^+ calculated at $r = 1.0$ Å, $R = 0.54$ Å for radius $q = 0.5$ Å; Row 3: Panels(A–C) show results for HeH_2^+ calculated at $r = 1.0$ Å, $R = 1.0$ Å for radius $q = 0.5$ Å; Row 4: Panels (A–C) show results for HeH_2^+ calculated at $r = 1.0$ Å, $R = 1.0$ Å for radius $q = 0.7$ Å; The panels (1A, 2A, 3A, 4A) represent three adiabatic potential energy curves (APECs), $u_i(R|r), i = 1$–3, as a function of R for fixed $r = 1.0$ Å. The panels (1B, 2B, 3B, 4B) display the two relevant NACTs $\boldsymbol{\tau}_{12}(\phi|q, s)$ and $\boldsymbol{\tau}_{23}(\phi|q, s)$ as a function of ϕ, calculated for circles with centres located at $R = 0.54$ Å and $R = 1.0$ Å. The panels (1C, 2C, 3C, 4C) depict the two relevant ADT angles $\boldsymbol{\gamma}_{12}(\phi|q, s)$ and $\boldsymbol{\gamma}_{23}(\phi|q, s)$ as a function of ϕ and the relevant(printed) topological phases α_{ij}.

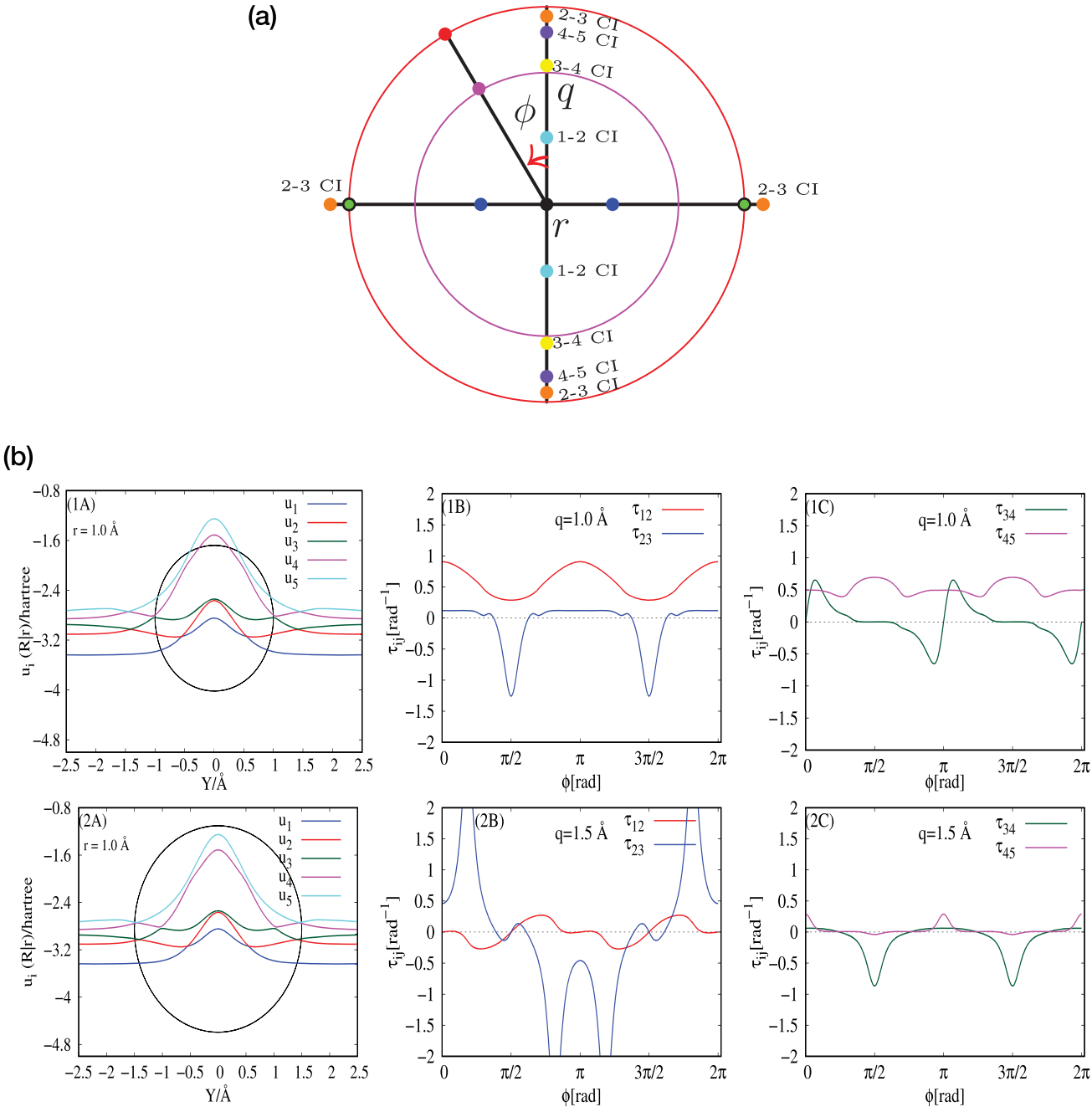

Figure 4. (a) The contour generation for HeH_2^+ system with the centre at $r = 1.0$ Å, $R = 0.0$ Å for $q = 1.0$ Å (inner circle) and 1.5 Å (outer circle). While the position of the two hydrogen atoms separated by a distance r is indicated by two solid circles along the X-axis, the position of the He atom is shown by solid circles on the two circular contours, along a line subtending an angle φ from the Y-axis. The approximate positions of the minima of the HeH_2^+ PES are at $X = 1.5$ Å, $Y = 0.0$ and $X = -1.5$ Å, $Y = 0.0$, where $X = R\cos\theta$ and $Y = R\sin\theta$ with $\theta = 0$ and π. A total of ten *ci* points shown in this figure are: two symmetric collinear (2,3) *cis* at ($X = 1.58$ Å, $Y = 0.0$ Å) and ($X = -1.58$ Å, $Y = 0.0$ Å); two symmetric C_{2v} (1,2) *cis* at ($X = 0.0$ Å, $Y = 0.54$ Å) and ($X = 0.0$ Å, $Y = -0.54$ Å); two symmetric C_{2v} (2,3) *cis* at ($X = 0.0$ Å, $Y = 1.45$ Å) and ($X = 0.0$ Å, $Y = -1.45$ Å); two symmetric C_{2v} (3,4) *cis* are at ($X = 0.0$ Å, $Y = 1.01$ Å) and ($X = 0.0$ Å, $Y = -1.01$ Å); two symmetric C_{2v} (4,5) *cis* at ($X = 0.0$ Å, $Y = 1.42$ Å) and ($X = 0.0$ Å, $Y = -1.42$ Å). (b) Row 1: Panels (A–C) show results for HeH_2^+ calculated at $r = 1.0$ Å, $R_{ce} = 0.0$ Å for radius $q = 1.0$ Å; Row 2: Panels (A–C) show results for HeH_2^+ calculated at $r = 1.0$ Å, $R = 0.0$ Å for radius $q = 1.5$ Å; The panels (1A, 2A) represent five adiabatic potential energy curves (APECs), $u_i(R|r)$, $i = 1$–5, as a function of Y coordinate ($Y = R\sin\theta$, where $\theta = \pi/2$ and $3\pi/2$) for fixed $r = 1.0$ Å. The panels (1B, 2B) display the two relevant NACTs $\boldsymbol{\tau}_{12}$ $(\phi|q, s)$ and $\boldsymbol{\tau}_{23}$ $(\phi|q, s)$ as a function of ϕ, calculated for circles with centres located at $R = 0.0$ Å with $q = 1.0$ Å and 1.5Å. The panels (1C, 2C) depict the other two relevant NACTs $\boldsymbol{\tau}_{34}$ $(\phi|q, s)$ and $\boldsymbol{\tau}_{45}$ $(\phi|q, s)$ as a function of ϕ calculated for circles with centres located at $R = 0.0$ Å with $q = 1.0$ Å and 1.5 Å.

3. Relation between NACTs and friction

The basic classical equation of motion which contains the friction term, $\beta\dot{x}$, takes the form [42,43]

$$m\ddot{x} + \beta(x)\dot{x} + \frac{\mathrm{d}V(x)}{\mathrm{d}x} = 0, \tag{4}$$

where $\dot{x}$ and $\ddot{x}$ stand for $(\mathrm{d}x/\mathrm{d}t)$ and $(\mathrm{d}^2x/\mathrm{d}t^2)$ respectively. In the present study we assume the friction coefficient to be x-dependent (in contrast to the available treatments in the literature [42,43]).

To make sense of the present treatment we try to reveal in what way the classical equation Equation (1) and the quantum mechanical equation Equation (3) are similar. This may not be a trivial task since Equation (3) is an equation where the unknown variables are matrices whereas Equation (1) is for scalar functions.

Still such a similarity can be achieved in case the study is carried out close enough to a *ci*-point. In this situation the BOH treatment can be satisfactorily carried out with two states only which means that it is enough to consider 2×2 matrices. Several years ago Baer and Englman [33, 114] and later on, Baer *et al.* [115,116] and Adhikari *et al.* [117,118] showed that for low enough (kinetic) energies the resulting two coupled BOH equations can be further reduced to become a single BOH equation which differs from the ordinary BO equation as it contains the relevant NACT(τ_{12}). This equation can be written for the present single translational coordinate R as:

$$-\frac{1}{2m}\left(\hbar\frac{\partial}{\partial R} + i\hbar\boldsymbol{\tau_{12}}(R)\right)^2 \boldsymbol{\Psi}(R) + (\boldsymbol{u_1}(R) - E)\,\boldsymbol{\Psi}(R) = \mathbf{0}, \tag{5}$$

where $\boldsymbol{u_1}(R)$ is the corresponding lowest potential energy curve (PEC).

It is important to emphasise that $\tau_{12}(R)$, in Eq. (5), is identified either with the angular NACT $\tau_{12}(\phi|q = R - R_0)$ (where ϕ is either 0 or π) or with an average value based on angular NACTs along a closed contour (details are given below).

Equation (5) is now, finally, presented in the appropriate form to be compared with Equation (2). In particular, we form a direct comparison between the kinetic terms of the two equations which is seen to reveal the relation between the above mentioned NACT term, $\tau_{12}(R)$ and the coefficient, $\beta(R)$ of the dissipative force (friction):

$$\hbar\tau_{12}(R) = \beta(R)(R - R_0) \Rightarrow \beta(R) = \frac{\hbar\tau_{12}(R)}{R - R_0}. \tag{6}$$

This result implies that $\beta(R)$ is dominated by a singularity of order higher than one (1) because $\tau_{12}(R)$ forms an ordinary pole at $R = R_0$. In other words we should accept the idea that $\beta(R)$ behaves at the vicinity of the quantum mechanical singularity as a pole of the second order namely being proportional to $(R - R_0)^{-2}$ or more explicitly:

$$\beta(R) = \frac{\hbar\left\langle\eta_1(\phi|R - R_0)|\frac{\partial}{\partial\phi}\eta_2(\phi|R - R_0)\right\rangle}{(R - R_0)^2}. \tag{7}$$

Here $\eta_j(\phi|R - R_0); j = 1, 2$ are the two corresponding electronic eigenfunctions and ϕ as mentioned earlier, is zero (0) or π (see also Figure 1).

Another way to treat Equation (6) is to replace $\tau_{12}(R)$ by its average value $\tilde{\tau}_{12}(R)$ along a closed contour:

$$\tilde{\tau}_{12}(R) = \oint (R - R_0)\tau_{12}(\phi|R)d\phi. \tag{8}$$

In case the two states are isolated at the considered CS, $\tilde{\tau}_{12}(R)$ becomes quantised namely [33]:

$$\tilde{\tau}_{12}(R) = n\pi \tag{9}$$

where n is an integer (or zero) and consequently $\beta(R)$ becomes:

$$\beta(R) = \frac{n\pi\hbar}{R - R_0}. \tag{10}$$

In this case $\beta(R)$ is seen to have a simple pole at R_0.

There is one issue which may play a role in favour of $\tau_{12}(R)$ being associated with the friction process:

A typical feature which characterises various friction processes is that during the slowing down process it produces energy as heat. In the present case if energy loss is created it is most likely created as light or, better, as photons a feature that is believed to be detected, for instance, during the production of HeH^+.

Another fact to be noticed is that since the NACTs frequently become singular implies that the BOH friction, whether to follow from Equation (6) or (9), may attain infinite large intensities and therefore could be rated among the *stronger* friction forces in the universe.

3.1. Extension to the complex plane

3.1.1. Treating complex NACTs

Since the NACTs become singular at the *ci*-points, one way to overcome this numerical difficulty (along the contour) is to shift slightly the contour by a negligible amount: $i\epsilon$, into the complex plane. The implications of this exercise, are discussed next for the simpler case in Equation (6):

In general:

$$\beta(R) = \frac{\hbar\tau(R)}{R - R_0 + i\epsilon} = \frac{\hbar\tau(R)}{(R - R_0)^2 + \epsilon^2}(R - R_0 - i\epsilon). \tag{11}$$

Next we define δR as

$$\delta R = R - R_0 \tag{12}$$

and continue by analysing two situations: (a) $\delta R >> \epsilon$

$$\beta(R) = \hbar\tau(R)\left(\frac{1}{R - R_0} - i\epsilon\frac{1}{(R - R_0)^2}\right) \tag{13}$$

(b) $\delta R << \epsilon$

$$\beta(R) = \hbar\tau(R)\left(\frac{R - R_0}{\epsilon^2} - \frac{i}{\epsilon}\right) \tag{14}$$

Thus combining the two possibilities we have:

$$\beta(R) = \begin{cases} \dfrac{\hbar\tau(R)}{R - R_0} : \delta R >> \epsilon, & \text{(far from } ci - \text{point)} \\ -i\dfrac{\hbar\tau(R)}{\epsilon} : \delta R << \epsilon, & \text{(close to } ci - \text{point)} \end{cases} \tag{15}$$

3.1.2. The complex equation of motion

Assuming:

$$R = R_1 + iR_2; \beta = \beta_1 + i\beta_2 \tag{16}$$

we get that Equation (4) takes the form:

$$m(\ddot{R}_1 + i\ddot{R}_2) + (\beta_1 + i\beta_2)(\dot{R}_1 + i\dot{R}_2) + \frac{\mathrm{d}V(R_1)}{dR_1} = 0. \tag{17}$$

Next are formed the resulting two coupled equations:

$$m\ddot{R}_1 + (\beta_1\dot{R}_1 - \beta_2\dot{R}_2) + \frac{\mathrm{d}V(R_1)}{dR_1} = 0, \tag{18a}$$

and

$$m\ddot{R}_2 + (\beta_2\dot{R}_1 + \beta_1\dot{R}_1) = 0, \tag{18b}$$

where following Equation (14), we get:

$$\beta_1(R_1) = \frac{\hbar\tau(R_1)}{(R_1 - R_0)^2 + \epsilon^2}(R_1 - R_0),$$
$$\beta_2(R_1) = -\frac{\hbar\tau(R_1)}{(R_1 - R_0)^2 + \epsilon^2}\epsilon. \tag{19}$$

In this study, we have considered the magnitude of ϵ as 0.01.

4. Computational details

In this paper, we have considered HeH_2^+ as a prototype triatomic system to demonstrate that NACTs can act as friction force during its formation. As it was mentioned earlier, the potential minimum occurs at a collinear configuration with $r = 1.0$ Å and $R = 1.55$ Å. In the nearby region in the nuclear CS, the first and second excited states of HeH_2^+ form a *ci* at $r = 1.0$ Å and $R = 1.58$ Å in the collinear rearrangement. It is important to add that HeH_2^+ forms (1,2) and (2,3) *cis* along C_{2v} configuration at $r = 1.0$ Å, $R = 0.54$ Å and $r = 1.0$ Å, $R = 1.45$ Å, respectively [27,119]. Therefore, we have explored its formation along collinear and C_{2v} configurations.

We have calculated the adiabatic PECs and NACTs of HeH_2^+ along the Jacobi coordinate R of collinear (see Figure 5(a)) and C_{2v} configurations keeping r fixed at 1.0 Å. In addition, we have calculated the same quantities along axes parallel to the collinear line shifted by distances, $\Delta = 0.3$, 0.4 and 0.5 Å (see Figure 5(b)). All ab initio calculations have been carried out using the quantum chemistry package MOLPRO[45], as described earlier, but with the aug-cc-pVQZ basis set including s, p, d and f functions for the H and He atoms. In SA-MCSCF calculations, the lowest three doublet electronic states, 1^1A_1, 2^1A_1, 3^1A_1 were state-averaged with equal weights. Subsequently, MR-CISD has been invoked with reference configurations generated from orbital spaces optimised through SA-MCSCF. The NACT between 2^1A_1 and 3^1A_1 states (τ_{23} ($\phi = 0|q = |R - R_0|$) has been calculated using the numerical finite differences, DDR method implemented in MOLPRO. Along the C_{2v} axis, only SA-MCSCF calculations are employed.

Since the system HeH_2^+ does not possess a (1,2) *ci* near the vicinity of the ground state potential minimum in the collinear arrangement, we have invoked τ_{23} to illustrate its friction effect on the formation of HeH_2^+. However, HeH_2^+ exhibits both (1,2) and (2,3) *cis* in C_{2v} configurations, as a result of which the NACTs τ_{12} as well as τ_{23} have been employed to understand the role of NACTs as a source of friction force.

In panels (a–d) of Figure 6, we have presented the lowest three PECs of HeH_2^+ as functions of R for $r = 1.0$ Å along the collinear axis and its parallel shifted axes. Figure 7(a–d) exhibit the ab-initio calculated NACT profiles along the collinear axis and the parallel shifted cases. Along the collinear axis, the 2nd and 3rd states are very close to each other and form avoided crossings at more than one configuration. As a result, τ_{23} ($\phi = 0|q = |R - R_0|$) in Figure 7(a) displays two peaks. It is evident from Figure 7 that as we move away from the collinear line, two of the three peaks of τ_{23} ($\phi = 0|q =$

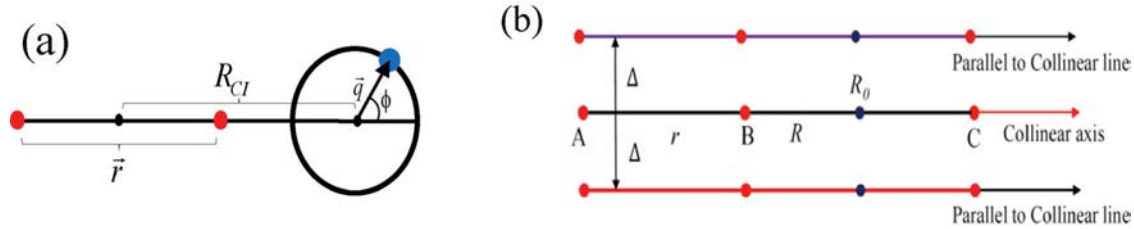

Figure 5. Schematic diagram of (a) the location of *ci* at $R = R_{ci}$ for the collinear geometry and the coordinates used for the calculation of the NACTs and (b) the coordinate system for the collinear axis (middle line) and the parallel cases. Δ indicates the separation of the parallel axis from the collinear line.

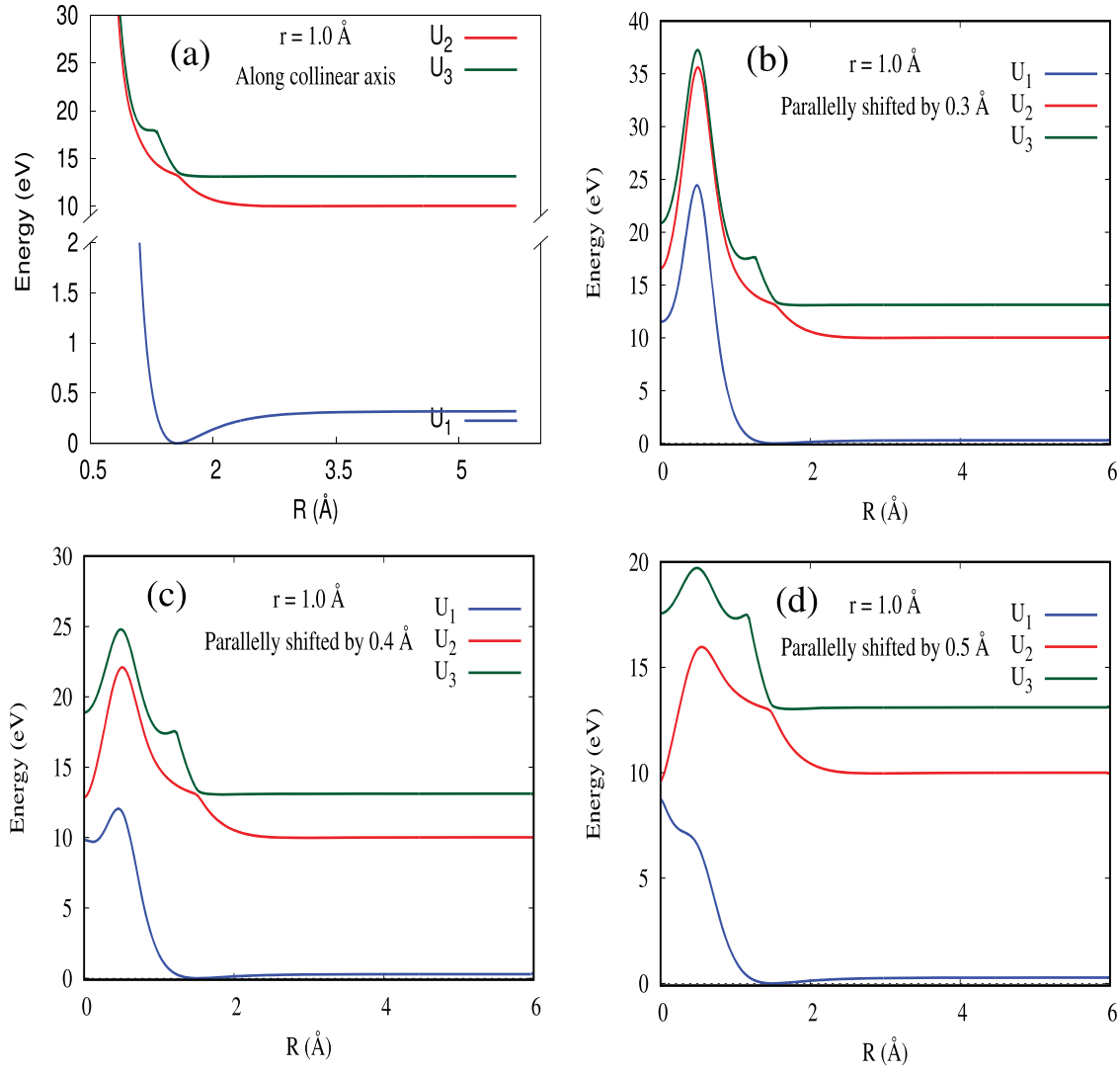

Figure 6. The adiabatic potential energy curves for the lowest three singlet states of HeH_2^+ along (a) collinear-axis; an axis parallel shifted from the collinear-axis by $\Delta =$ (b)0.3 Å; (c) 0.4 Å; (d) 0.5 Å. The energies are scaled with respect to the minimum of the ground state PEC along each trajectory.

$|R - R_0|$) gradually decrease. It is important to note that $\tau_{23}(\phi = 0|q = |R - R_0|)$ is singular at the ground state minimum of HeH_2^+ and thereby, could provide infinitely large frictional intensity at the potential well facilitating the trapping of the incoming atom (He) towards the diatomic ion (H_2^+).

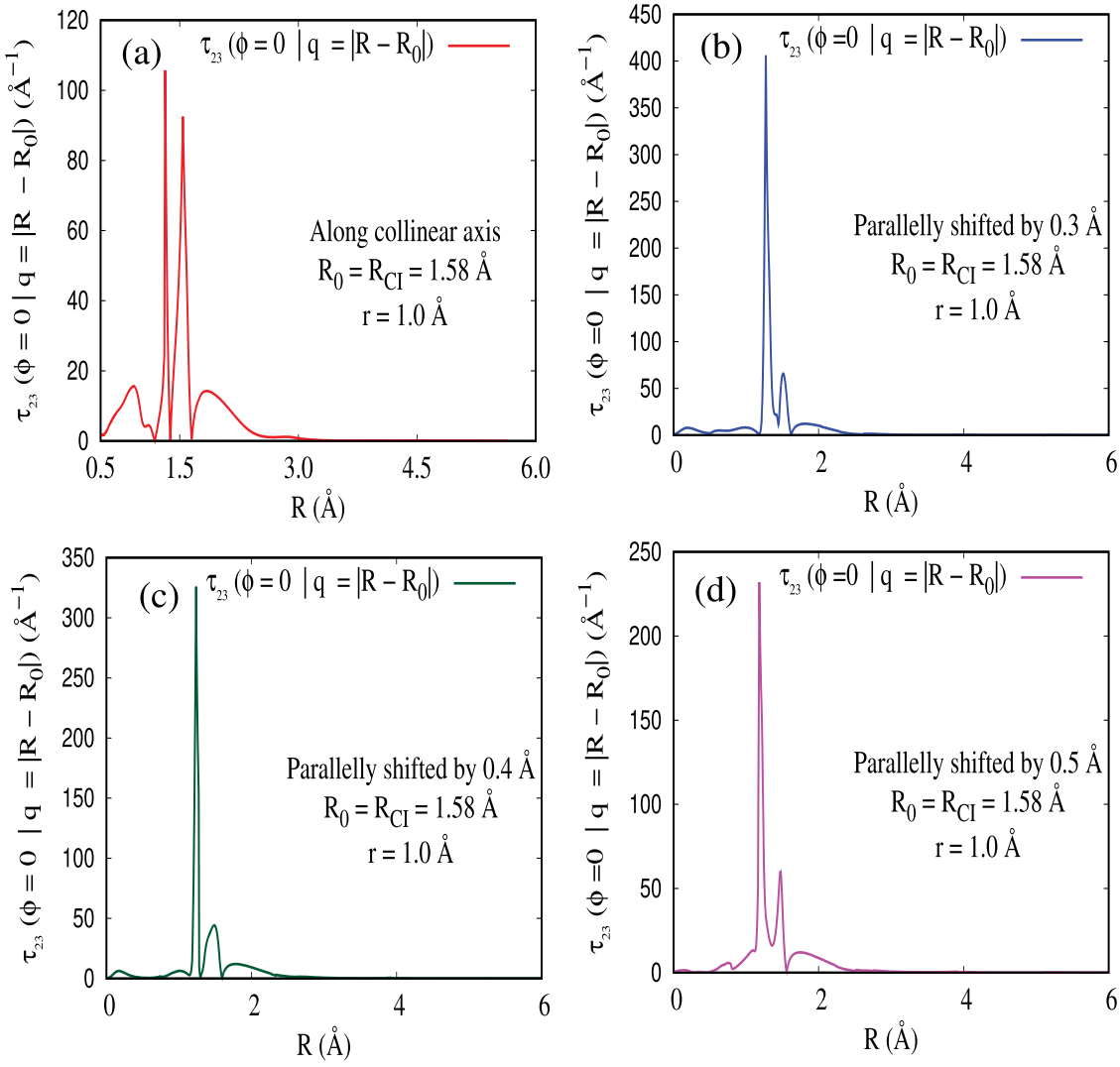

Figure 7. The NACT between two excited states (τ_{23} ($\phi = 0|q = |R - R_0|$)) for fixed value of $r = 1.0$ Å along (a) collinear-axis and an axis parallel shifted from the collinear-axis by $\Delta =$ (b)0.3 Å; (c) 0.4 Å; (d) 0.5 Å.

In Figure 8 are reproduced for ease of viewing, from Figure 3 A panels, the lowest three PECs of HeH_2^+ as functions of R for $r = 1.0$ Å along the C_{2v} axis. Included as an inset therein is the potential energy curve for the ground state showing a shallow well for the C_{2v} geometry.

The panels (a) and (b) of Figure 9 show the ab-initio calculated NACTs between 1^1A_1 and 2^1A_1 (τ_{12} ($\phi = 0|q = |R - R_0|$)) and 2^1A_1 and 3^1A_1 (τ_{23} ($\phi = 0|q = |R - R_0|$)) along the C_{2v} axis. These figures show clearly that HeH_2^+ forms (1,2) *ci* and (2,3) *ci* at $R = 0.54$ Å and $R = 1.45$ Å, respectively. It is important to note from Figure 8 that the ground adiabatic PES has a well depth of 0.09 eV along C_{2v} configuration, which is very small when compared to the collinear case (0.34 eV). Despite a very small potential well along the C_{2v} axis, the singular nature of NACTs could provide immense frictional force to impede the motion of the incoming atom (He) towards the diatom (H_2^+).

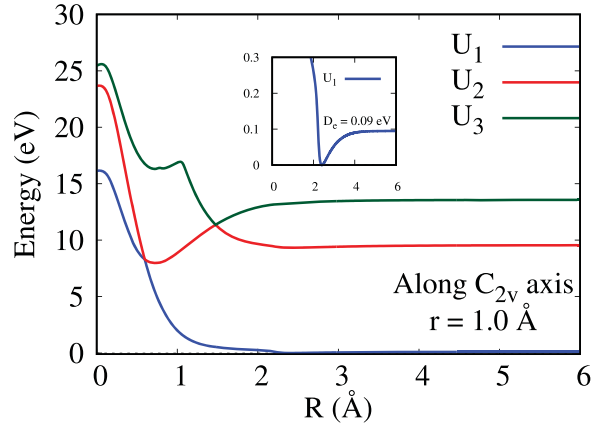

Figure 8. The adiabatic potential energy curves for the lowest three doublet states of HeH_2^+ for a fixed r value of 1.0 Å along the C_{2v} axis. The inset shows a magnified plot of the ground state adiabatic PEC near the minimum.

4.1. Classical dynamics results along collinear configuration

In this section we present quasi-classical trajectory calculations for the collision of H_2^+ and He starting with low initial kinetic energy (KE) to higher ones to explore the formation of HeH_2^+. The classical equation of motion (Equation (18)) containing the friction coefficient (β) is solved as discussed in Ref [44].

The *ab-initio* calculated ground state potential energy curve and the angular component of NACT have been invoked in the complex coupled classical equations of motion (Equation (18)), which are solved along the collinear as well as parallelly shifted trajectories. Since the differential equations involve singular NACTs, they have been solved using a stiff differential equation integrator, namely LSODE subroutine [120]. While solving those equations, the following initial conditions were employed: $R_1(t=0) = R_2(t=0) = 100$ Å with various initial KE values, namely, 1, 20, 50 and 500 eV. The initial values of the real and imaginary components of the velocity are defined as:

$$\dot{R}_1(t=0) = \sqrt{\frac{2\,KE(t=0)}{m}},$$
$$\dot{R}_2(t=0) = 0, \tag{20}$$
$$m = \sqrt{\frac{m_1 m_2 m_3}{m_1 + m_2 + m_3}},$$

where $m(= 0.8165$ amu) is the triatomic reduced mass of HeH_2^+.

We define the triatomic system in such a way that the diatomic moiety (H_2^+) is fixed at $r = 1.0$ Å and the third incoming atom (He) approaches collinearly from the asymptote with the above mentioned initial KE values along the collinear line or along any of the parallel shifted axes (see Figure 5(b)). The He atom may get trapped close to H_2^+ at its minimum due to either of the following two reasons or both: (a) The KE of the ion is insufficient to overcome the potential repulsion between H and He atoms; (b) Along the trajectory, the friction is so large that the incoming particle dissipates all its KE.

It may be noted that since the potential energy of the triatomic molecular ion is set to zero at its minimum, the kinetic energy of the species attains the same value (0) in case the trajectory of the incoming proton is trapped at that point (minimum energy of PEC).

In Table 1, we present the losses in KE values for an initial KE of 1, 20, 50 and 500 eV along the collinear axis and its parallelly shifted axis by $\Delta = 0.3$, 0.4 and 0.5 Å. For low enough initial KE of 1 eV, the KE loss is 100 % along collinear as well as parallelly shifted trajectories. This is attributed to the fact that the incoming He atom cannot overcome the high potential repulsion between H and He atoms and the friction (τ_{23} ($\phi = 0|q = |R - R_0|$)) is very large at the potential well. At initial KE value of 20 eV, the KE loss is again 100%, which means once again that the He atom gets trapped while moving along the collinear axis as well as along parallelly shifted trajectory. Here, the friction has a predominant role in stopping the incoming He atom since the barrier at the diatomic axis ($\sim$ 10 eV) is quite low as compared to the KE of the particle. At an initial KE value of 50 eV also, the particle gets trapped while moving along the collinear axis as well as along a trajectory shifted parallel from it by 0.3 Å. Similar to the 20 eV case, friction plays a major role in stopping the ion due to a low potential barrier as compared to the initial KE value. On the other hand, when the parallel trajectory is shifted by distances of 0.4 and 0.5 Å, the KE loss is 99.9% and 94.8%, respectively. Therefore, the friction is just not enough to hold the particle inside the potential well and it travels indefinitely to the other side of the collinear axis with a very small KE value. For a high KE value of 500 eV, the particle gets trapped only along the collinear trajectory since the two peaks of NACT of equal height (panel (a) of Figure 7) are able to provide the largest friction in this situation. For any of the parallel shifted trajectories, the friction is not enough to hold the particle inside the potential well.

In order to get a better understanding of these KE losses in Figure 10 we display the energy terms, namely potential energy and total energy of the system as functions of time in two different columns, A and B, respectively for a few representative cases. In the same figure, rows I and II depict results for dynamics carried out with initial KE = 20 eV along the collinear axis and along 0.5 Å parallel shifted trajectories, respectively. On the other hand, rows III and IV exhibit similar results

Table 1. The losses of kinetic energy in absolute magnitude and percentage loss are shown along collinear axis and its parallelly shifted cases for an initial KE 1 eV, 20 eV, 50 eV and 500 eV.

	1 eV		20 eV		50 eV		500 eV	
	Loss in KE	% loss	Loss in KE	% loss	Loss in KE	% loss	Loss in KE	% loss
Collinear axis	1	100	20	100	50	100	500	100
$\Delta = 0.3$ Å	1	100	20	100	50	100	373.9	74.7
$\Delta = 0.4$ Å	1	100	20	100	49.9	99.9	255.4	51.1
$\Delta = 0.5$ Å	1	100	20	100	47.4	94.8	212.8	42.5

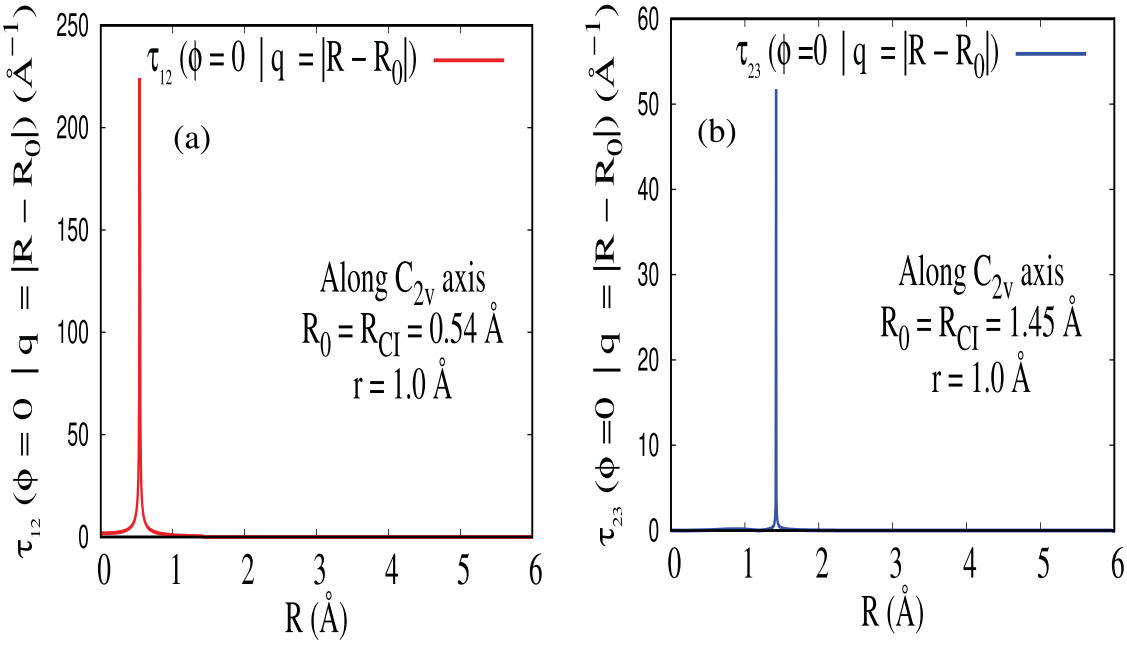

Figure 9. The NACTs between the ground electronic state and the first excited electronic state ($\boldsymbol{\tau}_{12}$ ($\phi = 0|q = |R - R_0|$); (b): The NACTs between the first and the second excited electronic states ($\boldsymbol{\tau}_{23}$ ($\phi = 0|q = |R - R_0|$).

for an initial KE of 500 eV. There are a few interesting observations that can be made from the above figure, which are directly correlated with the KE losses: (1) Panels I (A–B): At low initial KE (20 eV), the incoming proton gets trapped at the potential minimum while moving along the collinear axis owing to the fact that it cannot overcome the high potential barrier at the diatomic axis and the friction (τ_{23} ($\phi = 0|q = |R - R_0|$)) is very large at the potential well (see Figure 7). Thus, the potential and the total energies of the particle are dissipated to form a stable tri-atomic species; (2) Panels II(A–B): If the trajectory is shifted parallel from the collinear axis (by 0.5 Å), the NACT magnitude decreases substantially (see Figure 7(d)) and thereby, the effect of friction force reduces. Nevertheless, the friction is still enough to stop the ion, which gets trapped at the potential well due to insufficient energy to overcome the diatomic barrier (see Figure 6(d)); (3) Panels III(A–B): At very high KE (500 eV), it is the large magnitude of NACT acting as friction, which is solely responsible for trapping the ion inside the potential well while moving along the collinear trajectory; (4) Panels IV(A–B): The shift of the trajectory from the collinear line reduces the friction substantially, thus, failing to stop the ion moving with high initial KE of 500 eV at the potential well.

Hence, it can be concluded that the losses in KE can be directly correlated with the friction force due to the singularities in the NACT profiles facilitating the formation of HeH_2^+.

4.2. Classical dynamics results along C_{2v} configuration

In this section, we explore the possibility of formation of HeH_2^+ by quasi classical trajectory calculation for the collision process of H_2^+ and He along the C_{2v} axis. The classical equation of motion is solved along the lines discussed in Section 4.1. To solve the classical equation (Equation 18), we have employed the same initial conditions as earlier: $R_1(t = 0) = R_2(t = 0) = 100$ Å with initial KE = 1, 20, 50 and 500 eV.

To understand the frictional role of NACTs along the C_{2v} axis, we have performed two separate quasi-classical trajectory calculations by using τ_{12} ($\phi = 0|q = |R - R_0|$) and τ_{23} ($\phi = 0|q = |R - R_0|$) with different initial KE values mentioned above.

In Table 2, we summarise the loss in KE values along the C_{2v} axis with an initial KE of 1, 20, 50 and 500 eV. Two rows of Table 2 show the results obtained by using two NACTs (τ_{12} ($\phi = 0|q = |R - R_0|$) and τ_{23} ($\phi = 0|q = |R - R_0|$), respectively. For low enough KE of 1 eV, the loss in KE due to two NACTs is found to be 1% and 56%, respectively. Therefore, even for the lowest initial KE used, the particle is not trapped at the minimum due to the small well depth (0.09 eV). For other higher initial KE values, the He atom is not trapped and KE loss is substantially small for $\tau_{12}(\phi = 0|q = |R - R_0|)$ cases and smaller for $\tau_{23}(\phi = 0|q = |R - R_0|)$ cases.

It may be noted that the NACT is localised in the vicinity of the minimum in the collinear configuration,

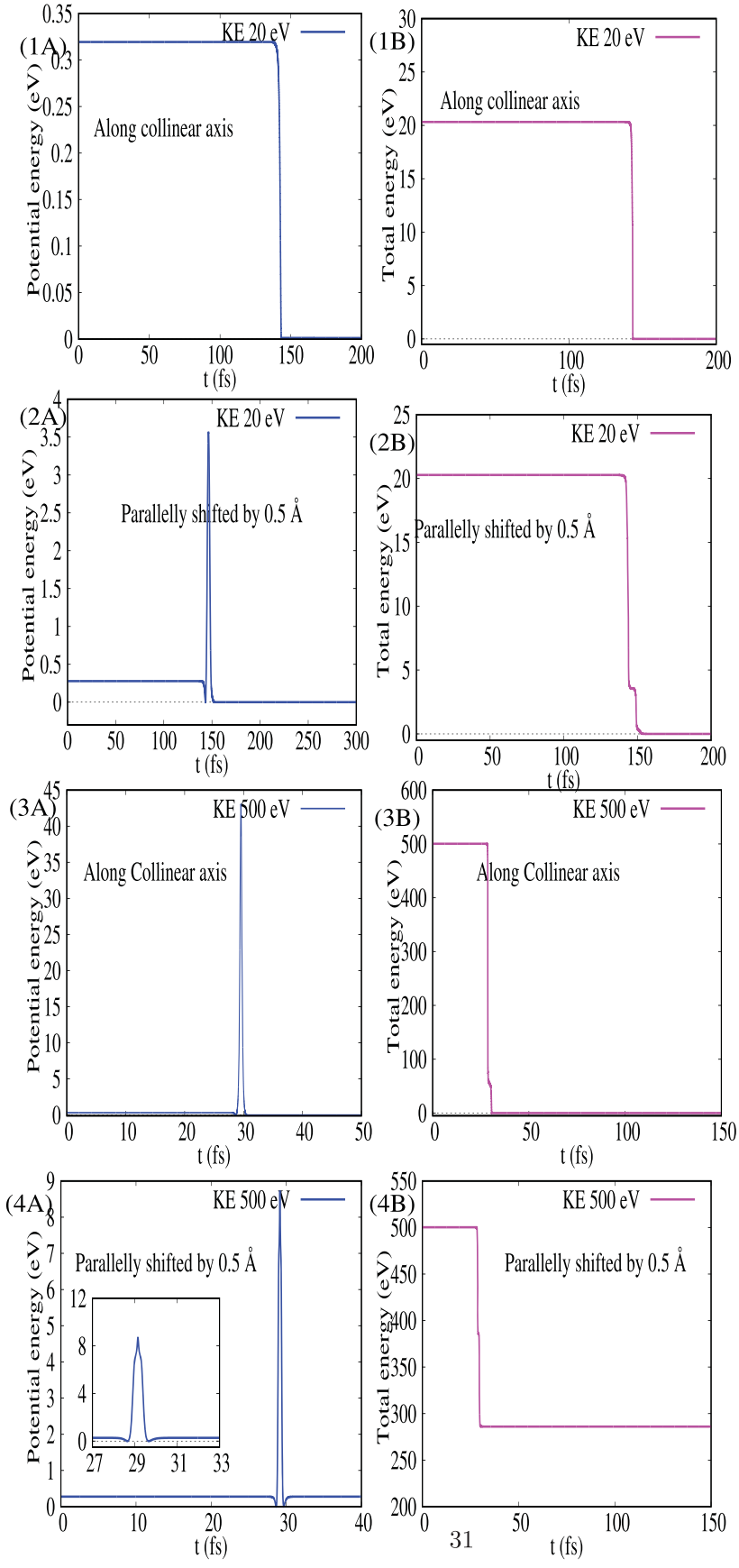

Figure 10. Plots of potential energy (Panels A), and total energy (Panels B) as a function of time (t) along the collinear axis and parallel axis shifted by 0.5 Å. Panels 1 and 2 show results along collinear and parallel shifted axis, respectively, for an initial KE of 20 eV. Panels 3 and 4 depict similar results for an initial KE $=$ 500 eV.

Table 2. The losses of kinetic energy in absolute magnitude and percentage loss are shown along the C_{2v} axis for an initial KE 1 eV, 20 eV, 50 eV and 500 eV.

NACTs used	1 eV		20 eV		50 eV		500 eV	
	Loss in KE	% loss	Loss in KE	% loss	Loss in KE	% loss	Loss in KE	% loss
τ_{12}	0.01	1.0	12.7	63.4	42.7	85.4	375.0	75
τ_{23}	0.01	0.56	10.4	52.0	9.35	18.7	33.0	6.6

Note: The classical dynamics is performed by using $\boldsymbol{\tau}_{12}$ ($\phi = 0|q = |R - R_0|$) and $\boldsymbol{\tau}_{23}$ ($\phi = 0|q = |R - R_0|$).

whereas the position of the potential well and the singular NACTs are well separated in the C_{2v} case. This also makes a substantial difference, in addition to the size of potential well. Hence, the NACTs act as a frictional force in a more effective way in the collinear configuration than in C_{2v}.

It is important to point out that a quantum mechanical description of the dynamics around conical intersection(s) would include the effect of the geometric phase that arises in a natural fashion. Unfortunately, there does not seem to be any obvious way to include the geometric phase in a classical mechanical description adopted in this study.

5. Conclusion

In this article, we have demonstrated that the BOH-NACT can act as a dissipative force – friction – to facilitate the formation of a stable tri-atomic species like HeH_2^+ only along collinear, but not along C_{2v} configurations. The quantisation and uniform distribution of NACTs have indicated that HeH_2^+ is enriched with multiple *cis*. It is proposed that the dissipative feature of NACTs can enable the formation of HeH_2^+ by keeping the three quasi-ions (He, H, H^+) in close proximity to each other, which dissociates to $HeH^+ + H$. Therefore, among all reaction channels of dissociation of HeH_2^+, the most dominant pathway is considered to be:

$$(He + H + H)^+ \rightarrow [HeH_2^+]^* \rightarrow HeH^+ + H.$$

In order to illustrate the frictional feature of NACTs, the classical equation of motion is solved along collinear as well as parallel shifted trajectories for various initial kinetic energies. It has been shown that along the collinear axis, the presence of a singular BOH-NACT in the nuclear CS can facilitate the formation of stable tri-atomic species from particles moving with KE values as high as 500 eV. These results have profound implications for the formation of di- and triatomic species in the early universe, during the chemical synthesis epoch following the nucleosynthesis that followed the Big Bang.

Acknowledgments

Satyam Ravi and Bijit Mukherjee acknowledge Indian Association for Cultivation of Science, Kolkata for research fellowship. Soumya Mukherjee thanks the Council of Scientific and Industrial Research, New Delhi SPM-07/080(0250)/2016-EMR-I for a research fellowship. Satrajit Adhikari is thankful to Science and Engineering Research Board, New Delhi for research funding.

Disclosure statement

No potential conflict of interest was reported by the author(s).

Funding

This work was supported by Science and Engineering Research Board, New Delhi research funding through Project No. CRG/2019/00793.

ORCID

Satrajit Adhikari http://orcid.org/0000-0002-2462-4892
Narayanasami Sathyamurthy http://orcid.org/0000-0002-6402-2765

References

[1] C.M. Coppola, S. Longo, M. Capitelli, F. Palla, and D. Galli, Astrophys. J. Suppl. Seri. **193** (1), 7 (2011). doi:10.1088/0067-0049/193/1/7
[2] S. Bovino and D. Galli, Science **365** (6454), 639–639 (2019). doi:10.1126/science.aay5825
[3] D. Galli and F. Palla, Annu. Rev. Astron. Astrophys. **51** (1), 163–206 (2013). doi:10.1146/annurev-astro-082812-141029
[4] S. Bovino, M. Tacconi, F.A. Gianturco, and D. Galli, Astron. Astrophys. **529**, A140 (2011). doi:10.1051/0004-6361/201116740
[5] T.R. Hogness and E.G. Lunn, Phys. Rev. **26**, 44–55 (1925). doi:10.1103/PhysRev.26.44
[6] R. Güsten, H. Wiesemeyer, D. Neufeld, K. M. Menten, U. U. Graf, K. Jacobs, B. Klein, O. Ricken, C. Risacher, and J. Stutzki, Nature **568** (7752), 357 (2019). doi:10.1038/s41586-019-1090-x
[7] O. Novotný, P. Wilhelm, D. Paul, A. Kálosi, S. Saurabh, A. Becker, K. Blaum, S. George, J. Göck, M. Grieser, F. Grussie, R. von Hahn, C. Krantz, H. Kreckel, C. Meyer, P.M. Mishra, D. Muell, F. Nuesslein, D.A. Orlov, M. Rimmler, V.C. Schmidt, A. Shornikov, A.S. Terekhov, S. Vogel, D. Zajfman, and A. Wolf, Science **365**, 676 (2019). doi:10.1126/science.aax5921

[8] F. Palla, E.E. Salpeter, and S. W. Stahler, Astrophys. J. **271**, 632–641 (1983). doi:10.1086/161231

[9] S. Lepp, P.C. Stancil, and A. Dalgarno, J. Phys. B: Atomic Mol. Opt. Phys. **35** (10), R57–R80 (2002). doi:10.1088/0953-4075/35/10/201

[10] D.G. Hopper, J. Chem. Phys. **73**, 3289 (1980). doi:10.1063/1.440524

[11] D.G. Hopper, J. Chem. Phys. **73**, 4528 (1980). doi:10.1063/1.440691

[12] D.G. Hopper, J. Chem. Phys. **74**, 4218 (1981). doi:10.1063/1.441562

[13] B. Mukherjee, D. Mukhopadhyay, S. Adhikari, and M. Baer, Mol. Phys. **116** (19-20), 2435–2448 (2018). doi:10.1080/00268976.2018.1442940

[14] B. Mukherjee, D. Mukhopadhyay, S. Adhikari, and M. Baer, preprint ArXiv:1801.00103 (2018), [physics.chem-ph].

[15] B. Mukherjee, K.R. Shamasundar, S. Adhikari, and M. Baer, Int. J. Quantum Chem. **119** (16), e25949 (2019). doi:10.1002/qua.25949

[16] E. Zicler, O. Parisel, F. Pauzat, Y. Ellinger, M.C. Bacchus-Montabonel, and J.P. Maillard, Astron. Astrophys. **607**, A61 (2017). doi:10.1051/0004-6361/201731441

[17] A. Carrington, D.I. Gammie, A.M. Shaw, S.M. Taylor, and J.M. Hutson, Chem. Phys. Lett. **260** (3), 395–405 (1996). doi:10.1016/0009-2614(96)00860-3

[18] D.R. McLaughlin and D.L. Thompson, J. Chem. Phys. **70**, 2748 (1979). doi:10.1063/1.437861

[19] V. Spirko and W.P. Kraemer, J. Mol. Spectrosc. **172**, 265 (1995). doi:10.1006/jmsp.1995.1174

[20] M.F. Falcetta, Mol. Phys. **88**, 647 (1996). doi:10.1080/00268979650026190

[21] M.F. Falcetta and P.E. Siska, Mol. Phys. **97**, 117 (1999). doi:10.1080/00268979909482814

[22] M. Meuwly and J.M. Hutson, J. Chem. Phys. **110**, 3418 (1999). doi:10.1063/1.478208

[23] B. Maiti and N. Sathyamurthy, Chem. Phys. Lett. **345**, 461 (2001). doi:10.1016/S0009-2614(01)00902-2

[24] T. Szidarovszky and K. Yamanouchi, Mol. Phys. **115**, 1916 (2017). doi:10.1080/00268976.2017.1297863

[25] D. Papp, A.G. Császár, K. Yamanouchi, and T. Szidarovszky, J. Chem. Theo. Comput **14** (3), 1523 (2018). doi:10.1021/acs.jctc.7b01136

[26] D. Koner, J.C.S.V. Veliz, A. van der Avoird, and M. Meuwly, Phys. Chem. Chem. Phys. **21**, 24976 (2019). doi:10.1039/C9CP05259C

[27] A.K. Gupta, V. Dhindhwal, M. Baer, N. Sathyamurthy, S. Ravi, S. Mukherjee, B. Mukherjee, and S. Adhikari, Mol. Phys. **118**, e1683243 (2020). doi:10.1080/00268976.2019.1683243

[28] B. Maiti, S. Mahapatra, and N. Sathyamurthy, J. Chem. Phys. **113**, 59 (2000). doi:10.1063/1.481773

[29] "Quasi-ions are the particles to treated by the BOH equation - thus ions wrapped by an electronic cloud while moving in CS.".

[30] M. Born and R. Oppenheimer, Ann. Phys. **389** (20), 457–484 (1927). doi:10.1002/andp.19273892002

[31] M. Born, Festschrift Goett. Nach. Math. Phys. **K1**, 1–6 (1951).

[32] M. Born and K. Huang, *Dynamical Theory of Crystal Lattices* (Oxford University, New York, 1954).

[33] M. Baer, *Beyond Born-Oppenheimer: Electronic Non-adiabatic Coupling Terms and Conical Intersections* (John Wiley & Sons, Hoboken, N. J., 2006). (a) Sect 2.1.1; (b) Sect 3.2.2; (c) Sect. 2.1.3.3; (d) Sect. 2.1.3.2; (e) Sect. 6.2; (f) Sect. 3.2.4).

[34] M. Baer, Chem. Phys. Lett. **35** (1), 112–118 (1975). doi:10.1016/0009-2614(75)85599-0

[35] V. Dhindhwal, M. Baer, and N. Sathyamurthy, J. Phys. Chem. A **120** (19), 2999–3008 (2016). PMID: 26583700. doi:10.1021/acs.jpca.5b08921

[36] B. Mukherjee, K. Naskar, S. Mukherjee, S. Ghosh, T. Sahoo, and S. Adhikari, Int. Rev. Phys. Chem. **38** (3-4), 287–341 (2019). doi:10.1080/0144235X.2019.1672987

[37] K. Naskar, S. Mukherjee, B. Mukherjee, S. Ravi, S. Mukherjee, S. Sardar, and S. Adhikari, J. Chem. Theory. Comput. **16** (3), 1666–1680 (2020). doi:10.1021/acs.jctc.9b00948

[38] M. Gell-Mann, Phys. Lett. **8** (3), 214–215 (1964). doi:10.1016/S0031-9163(64)92001-3

[39] G. Zweig, CERN Report No. 8182/TH 401 (1964) .

[40] R. Baer, D.J. Kouri, M. Baer, and D.K. Hoffman, J. Chem. Phys. **119** (14), 6998–7002 (2003). doi:10.1063/1.1606433

[41] S. Adhikari and G.D. Billing, J. Chem. Phys. **107** (16), 6213–6218 (1997). doi:10.1063/1.474286

[42] H. Goldstien, *Classical Mechanics* (Addison-Wesley Publishing Company, Cambridge, Mass, 1956).

[43] L.D. Landau and E.M. Lifshitz, *Mechanics* (Elsevier, MA, 1997).

[44] S. Ravi, S. Mukherjee, B. Mukherjee, S. Adhikari, N. Sathyamurthy, and M. Baer, under review to EPJD (2020).

[45] H.-J. Werner, P.J. Knowles, G. Knizia, F.R. Manby, M. Schütz, P. Celani, W. Györffy, D. Kats, T. Korona, R. Lindh, A. Mitrushenkov, G. Rauhut, K.R. Shamasundar, T.B. Adler, R.D. Amos, S.J. Bennie, A. Bernhardsson, A. Berning, D.L. Cooper, M.J.O. Deegan, A.J. Dobbyn, F. Eckert, E. Goll, C. Hampel, A. Hesselmann, G. Hetzer, T. Hrenar, G. Jansen, C. Köppl, S.J.R. Lee, Y. Liu, A.W. Lloyd, Q. Ma, R.A. Mata, A.J. May, S.J. McNicholas, W. Meyer, T.F. Miller III, M.E. Mura, A. Nicklass, D.P. O'Neill, P. Palmieri, D. Peng, K. Pflüger, R. Pitzer, M. Reiher, T. Shiozaki, H. Stoll, A.J. Stone, R. Tarroni, T. Thorsteinsson, M. Wang, and M. Welborn, MOLPRO, version 2018.2, a package of ab initio programs https://www.molpro.net/ (2018).

[46] M.V. Berry, Proc. R. Soc. London. A **392**, 45 (1984). doi:10.1098/rspa.1984.0023

[47] D.C. Clary, Science **309**, 1195–1196 (2005). doi:10.1126/science.1117201

[48] M.S. Child, Adv. Chem. Phys. **124**, 1 (2002). in *The Role of Degenerate States in Chemistry*, edited by I. Prigogine, S.A. Rice, M. Baer and G.D. Billing. doi:10.1002/0471433462.ch1

[49] M. Baer and R. Englman, Mol. Phys. **75**, 283 (1992). doi:10.1080/00268979200100231

[50] Z.H. Top and M. Baer, Chem. Phys. **25**, 1 (1977). doi:10.1016/0301-0104(77)87060-2

[51] M. Baer, G. Niedner-Schatteburg, and J.P. Toennies, J. Chem. Phys. **91**, 4169 (1989). doi:10.1063/1.456794

[52] R. Englman and T. Vèrtesi, J. Phys. B: At. Mol. Opt. Phys. **38**, 2443 (2005). doi:10.1088/0953-4075/38/14/009

[53] E. Bene, T. Vèrtesi, and R. Englman, J. Chem. Phys. **135**, 084101 (2011). doi:10.1063/1.3625917

[54] R. Englman, J. Chem. Phys. **144**, 024103 (2016). doi:10.1063/1.4939243

[55] J. Meisner, M. Vacher, M.J. Bearpark, and M.A. Robb, J. Chem. Theory Comput. **11**, 3115 (2015). doi:10.1021/acs.jctc.5b00364

[56] G.J. Halász, A. Vibók, A.M. Mebel, and M. Baer, J. Chem. Phys. **118** (7), 3052–3064 (2003). doi:10.1063/1.1536925

[57] H.C. Longuet-Higgins, in *Advances in Spectroscopy* (1961), p. 429 .

[58] F.T. Smith, Phys. Rev. **179** (1), 111 (1969). doi:10.1103/PhysRev.179.111

[59] E.J. Brändas and P. Froelich, Int. J. Quantum. Chem. **13** (5), 619–626 (1978). doi:10.1002/qua.560130506

[60] C.A. Mead and D.G. Truhlar, J. Chem. Phys. **77** (12), 6090–6098 (1982). doi:10.1063/1.443853

[61] H.-J. Werner, B. Follmeg, and M.H. Alexander, J. Chem. Phys. **89** (5), 3139–3151 (1988). doi:10.1063/1.454971

[62] C. Petrongolo, G. Hirsch, and R.J. Buenker, Mol. Phys. **70** (5), 825–834 (1990). doi:10.1080/00268979000101381

[63] G. Hirsch, R.J. Buenker, and C. Petrongolo, Mol. Phys. **70** (5), 835–848 (1990). doi:10.1080/00268979000101391

[64] D.R. Yarkony, J. Chem. Phys. **105** (23), 10456–10461 (1996). doi:10.1063/1.472972

[65] R.G. Sadygov and D.R. Yarkony, J. Chem. Phys. **109** (1), 20–25 (1998). doi:10.1063/1.476552

[66] E.S. Kryachko and D.R. Yarkony, Int. J. Quantum. Chem.**76** (2), 235–243 (2000). doi:10.1002/(SICI)1097-461X(2000)76:2 < 235::AID-QUA12 > 3.0.CO;2-Y

[67] T. Pacher, L. Cederbaum, and H. Köppel, Adv. Chem. Phys. **84**, 293–392 (1993) in *Advances in Chemical Physics*, edited by I. Prigogine and S.A. Rice. doi:10.1002/9780470141427.ch4.

[68] G.J. Tawa, S.L. Mielke, D.G. Truhlar, and D.W. Schwenke, J. Chem. Phys. **100** (8), 5751–5777 (1994). doi:10.1063/1.467140

[69] L.F. Errea, A. Macías, L. Méndez, I. Rabadán, A. Riera, A. Rojas, and P. Sanz, Phys. Rev. A **63**, 062713 (2001). doi:10.1103/PhysRevA.63.062713

[70] I.B. Bersuker, Chem. Rev. **101** (4), 1067–1114 (2001). doi:10.1021/cr0004411

[71] Z.R. Xu., M. Baer, and A.J. Varandas, J. Chem. Phys. **112** (6), 2746–2751 (2000). doi:10.1063/1.480848

[72] A. Vibok, G.J. Halasz, T. Vèrteśi, S. Suhai, M. Baer, and J. P. Toennies, J. Chem. Phys. **119** (13), 6588–6596 (2003). doi:10.1063/1.1601592

[73] B. Sarkar, S. Adhikari, and M. Baer, J. Chem. Phys. **127** (1), 014301 (2007). doi:10.1063/1.2743437

[74] B. Sarkar and S. Adhikari, J. Phys. Chem. A **112** (40), 9868–9885 (2008). doi:10.1021/jp8029709

[75] S. Mukherjee, S. Bandyopadhyay, A.K. Paul, and S. Adhikari, J. Phys. Chem. A **117** (16), 3475–3495 (2013). doi:10.1021/jp311597c

[76] S. Mukherjee, B. Mukherjee, S. Sardar, and S. Adhikari, J. Chem. Phys. **143** (24), 244307 (2015). doi:10.1063/1.4938526

[77] B. Mukherjee, S. Mukherjee, S. Sardar, K.R. Shamasundar, and S. Adhikari, Chem. Phys. **515**, 350–359 (2018). doi:10.1016/j.chemphys.2018.09.017

[78] C. Levi, G.J. Halász, Á. Vibók, I. Bar, Y. Zeiri, R. Kosloff, and M. Baer, J. Chem. Phys. **128** (24), 244302 (2008). doi:10.1063/1.2943143

[79] J. Larson and E. Sjöqvist, Phys. Rev. A. **79** (4), 043627 (2009). doi:10.1103/PhysRevA.79.043627

[80] A. Das and D. Mukhopadhyay, J. Phys. Chem. A **116** (7), 1774–1785 (2012). doi:10.1021/jp208684p

[81] A. Das and D. Mukhopadhyay, Chem. Phys. **412**, 51–57 (2013). doi:10.1016/j.chemphys.2012.12.007

[82] A. Das and D. Mukhopadhyay, J. Phys. Chem. A **117** (36), 8680–8690 (2013). doi:10.1021/jp403068v

[83] A. yang Yu, Phys. Chem. An Ind. J. **10** (1), 7–11 (2015).

[84] A. Das, D. Mukhopadhyay, S. Adhikari, and M. Baer, J. Chem. Phys.**133** (8), 084107 (2010). doi:10.1063/1.3479399

[85] J.E. Subotnik, R.J. Cave, R.P. Steele, and N. Shenvi, J. Chem. Phys. **130** (23), 234102 (2009). doi:10.1063/1.3148777

[86] S. Hammes-Schiffer, J. Phys. Chem. Lett. **2** (12), 1410–1416 (2011). doi:10.1021/jz200277p

[87] W. Skomorowski, F. Pawłowski, T. Korona, R. Moszynski, P.S. Żuchowski, and J.M. Hutson, J. Chem. Phys. **134** (11), 114109 (2011). doi:10.1063/1.3563613

[88] A. Yahalom, *Advances in Classical Field Theory* (Bentham, 2011). eBooks eISBN 978-1-608805- 195-3, Chap. 9. Ariel 40700, Israel.

[89] S. Al-Jabour, M. Baer, O. Deeb, M. Leibscher, J. Manz, X. Xu, and S. Zilberg, J. Phys. Chem. A **114** (9), 2991–3010 (2010). doi:10.1021/jp905038t

[90] T. Van Voorhis, T. Kowalczyk, B. Kaduk, L.-P. Wang, C.-L. Cheng, and Q. Wu, Annu. Rev. Phys. Chem. **61**, 149–170 (2010). doi:10.1146/annurev.physchem.012809.103324

[91] M.S. Kaczmarski, Y. Ma, and M. Rohlfing, Phys. Rev. B. **81** (11), 115433 (2010). doi:10.1103/PhysRevB.81.115433

[92] R. Baer, Phys. Rev. Lett. **104** (7), 073001 (2010). doi:10.1103/PhysRevLett.104.073001

[93] I. Ryb and R. Baer, J. Chem. Phys. **121** (21), 10370–10375 (2004). doi:10.1063/1.1808695

[94] T. Yonehara, K. Hanasaki, and K. Takatsuka, Chem. Rev. **112** (1), 499–542 (2012). doi:10.1021/cr200096s

[95] C. Hu, O. Sugino, and K. Watanabe, J. Chem. Phys. **135** (7), 074101 (2011). doi:10.1063/1.3624565

[96] R. Englman and T. Vértesi, J. Phys. B: Atom., Molecular Opt. Phys. **38** (14), 2443 (2005). doi:10.1088/0953-4075/38/14/009

[97] R. Englman, J. Chem. Phys. **144** (2), 024103 (2016). doi:10.1063/1.4939243

[98] M. Mitić, M. Milovanović, R. Ranković, S. Jerosimić, and M. Perić, Mol. Phys. **116** (19-20), 2671–2685 (2018). doi:10.1080/00268976.2018.1445876

[99] N.I. Gidopoulos and E.K.U. Gross, Philos. Trans. R. Soc. A: Math., Phys. Eng. Sci. **372** (2011), 20130059 (2014). doi:10.1098/rsta.2013.0059

[100] A. Abedi, N.T. Maitra, and E.K.U. Gross, Phys. Rev. Lett. **105** (12), 123002 (2010). doi:10.1103/PhysRevLett.105.123002

[101] A. Abedi, N.T. Maitra, and E.K.U. Gross, J. Chem. Phys. **137** (22), 22A530 (2012). doi:10.1063/1.4745836

[102] S. Belz, S. Zilberg, M. Berg, T. Grohmann, and M. Leibscher, J. Phys. Chem. A **116** (46), 11189–11198 (2012). doi:10.1021/jp305090b

[103] S. Al-Jabour and M. Leibscher, J. Phys. Chem. A **119** (2), 271–280 (2015). doi:10.1021/jp509604e
[104] M. Łabuda, J. González-Vázquez, F. Martín, and L. González, Chem. Phys. **400**, 165–170 (2012). doi:10.1016/j.chemphys.2012.03.019
[105] G.A. Worth and M. Robb, Adv. Chem. Phys. **124** (1), 355–432 (2002) in *The Role of Degenerate States in Chemistry*, edited by I. Prigogine, S.A. Rice, M. Baer and G.D. Billing. doi:10.1002/0471433462.ch7
[106] G.W. Richings and G.A. Worth, J. Phys. Chem. A **119** (50), 12457–12470 (2015). doi:10.1021/acs.jpca.5b07921
[107] C. Hu, R. Komakura, Z. Li, and K. Watanabe, Int. J. Quantum. Chem. **113** (3), 263–271 (2013). doi:10.1002/qua.24130
[108] E.N. Ghassemi, J. Larson, and Å. Larson, J. Chem. Phys. **140** (15), 154304 (2014). doi:10.1063/1.4871014
[109] I.G. Ryabinkin, C.Y. Hsieh, R. Kapral, and A.F. Izmaylov, J. Chem. Phys. **140** (8), 084104 (2014). doi:10.1063/1.4881147
[110] X. Liu and J.E. Subotnik, J. Chem. Theory. Comput. **10** (3), 1004–1020 (2014). doi:10.1021/ct4009377
[111] G.W. Richings and G.A. Worth, Chem. Phys. Lett. **683**, 606–612 (2017). doi:10.1016/j.cplett.2017.03.032
[112] G.W. Richings and S. Habershon, Chem. Phys. Lett. **683**, 228–233 (2017). doi:10.1016/j.cplett.2017.01.063
[113] E.J. Brändas, Mol. Phys. **116** (19-20), 2622–2632 (2018). doi:10.1080/00268976.2018.1471227
[114] M. Baer and R. Englman, Chem. Phys. Lett. **265** (1-2), 105–108 (1997). doi:10.1016/S0009-2614(96)01411-X
[115] R. Baer, D.M. Charutz, R. Kosloff, and M. Baer, J. Chem. Phys. **105** (20), 9141–9152 (1996). doi:10.1063/1.472748
[116] S. Adhikari, G.D. Billing, A. Alijah, S.H. Lin, and M. Baer, Phys. Rev. A. **62** (3), 032507 (2000). doi:10.1103/PhysRevA.62.032507
[117] B. Sarkar and S. Adhikari, J. Chem. Phys. **124** (7), 074101 (2006). doi:10.1063/1.2170089
[118] S. Mukherjee, B. Mukherjee, S. Sardar, and S. Adhikari, Comput. Theor. Chem. **1154**, 57–67 (2019). doi:10.1016/j.comptc.2019.03.011
[119] N. Sathyamurthy, M. Baer, S. Ravi, S. Mukherjee, B. Mukherjee, and S. Adhikari, preprint arXiv (2019), physics.chem-ph, arXiv:1912.11076v1 .
[120] A.C. Hindmarsh, Sci. Comput. **1**, 55–64 (1983).

Appendix

The basic classical equation of motion which contains the friction term, $\beta\dot{x}$, takes the form:

$$m\,\ddot{x} + \beta\,\dot{x} + \frac{\mathrm{d}V(x)}{\mathrm{d}x} = 0, \tag{A1}$$

where the terms $\dot{x}$ and $\ddot{x}$ stand for $(\mathrm{d}/\mathrm{d}t)x$ and $(d^2/\mathrm{d}t^2)x$ respectively.

Multiplying the equation by $\dot{x}$ we get:

$$m\ddot{x}\dot{x} + \beta\dot{x}^2 + \frac{\mathrm{d}V}{\mathrm{d}x}\dot{x} = 0. \tag{A2}$$

Next, introducing the explicit derivative with respect to time we get:

$$\frac{m}{2}\frac{\mathrm{d}}{\mathrm{d}t}\left(\dot{x}^2\right) + \frac{\mathrm{d}}{\mathrm{d}t}\left(\beta\dot{x}(x-x_0)\right) - (x-x_0)\left(\beta\ddot{x} + \dot{x}\frac{\mathrm{d}\beta}{\mathrm{d}t}\right) + \frac{\mathrm{d}V(x)}{\mathrm{d}t} = 0 \tag{A3}$$

or

$$\frac{\mathrm{d}}{\mathrm{d}t}\left[\left(\frac{m}{2}\dot{x}^2 + \beta\dot{x}(x-x_0)\right) + V(x)\right] = \beta(x-x_0)\ddot{x} + \frac{\mathrm{d}\beta}{\mathrm{d}t}(x-x_0)\dot{x}. \tag{A4}$$

Completing the squaring process for the l.h.s. and replacing $\ddot{x}$ on the r.h.s. of Equation A4 yields (see Equation A1):

$$\frac{\mathrm{d}}{\mathrm{d}t}\left[\frac{m}{2}\left(\dot{x} + \frac{1}{m}\beta(x-x_0)\right)^2 + V(x)\right] = -\frac{1}{m}\beta(x-x_0)\left(\beta\dot{x} + \frac{\mathrm{d}V(x)}{\mathrm{d}x}\right) + \frac{1}{2m}\frac{\mathrm{d}}{\mathrm{d}t}\left(\beta^2(x-x_0)^2\right) + \frac{\mathrm{d}\beta}{\mathrm{d}t}(x-x_0)\dot{x} \tag{A5}$$

or

$$\frac{\mathrm{d}}{\mathrm{d}t}\left[\frac{m}{2}\left(\dot{x} + \frac{1}{m}\beta(x-x_0)\right)^2 + V(x)\right] = F(x,\dot{x}) \tag{A6}$$

where,

$$F(x,\dot{x}) = (x-x_0)\left[-\frac{1}{m}\beta\frac{\mathrm{d}V}{\mathrm{d}x} + \frac{\mathrm{d}\beta}{\mathrm{d}t}\left(\frac{1}{m}\beta(x-x_0) + \dot{x}\right)\right]. \tag{A7}$$

In applications x_0 will be identified with the *ci*-point. It is well noticed that conservation of energy is maintained when friction disappears.